

# PROCEEDINGS OF SPIE

[SPIDigitalLibrary.org/conference-proceedings-of-spie](https://spiedigitallibrary.org/conference-proceedings-of-spie)

## Origins of Kerr phase and orientational phase in polymer-dispersed liquid crystal

Chia-Ming Chang  
Yi-Hsin Lin  
Victor Reshetnyak  
Chui Ho Park  
Ramesh Manda  
Seung Hee Lee

# Origins of Kerr Phase and Orientational Phase in Polymer-Dispersed Liquid Crystal

Chia-Ming Chang<sup>a</sup>, Yi-Hsin Lin<sup>\*a</sup>, Victor Reshetnyak<sup>b</sup>, Chui Ho Park<sup>c</sup>, Ramesh Manda<sup>c</sup> and Seung Hee Lee<sup>c</sup>

<sup>a</sup>Department of Photonics, National Chiao Tung University, Hsinchu 30010, Taiwan; <sup>b</sup>Theoretical Physics Department, Taras Shevchenko National University of Kyiv, Kyiv 01033, Ukraine;

<sup>c</sup>Department of BIN Convergence Technology and Department of Polymer Nano-Science and Technology, Chonbuk National University, Jeonju, Jeonbuk 561-756, Korea

## ABSTRACT

The anisotropic properties of nematic liquid crystals result in polarization dependency which leads to requirement of at least a polarizer in liquid crystal photonic devices. To develop polarizer free phase modulation, Kerr effect is one of the path. The phase modulation in polymer dispersed liquid crystals (PDLCs) is shown to have two parts: Kerr phase, which is the optical phase modulation linearly proportional to a square of electric field, and orientational phase. However, many puzzles are still under investigation: the origins of Kerr phase, the relation between Kerr phase and orientational phase, and how two-steps of electro-optical (EO) response relates to Kerr phase and orientational phase. We investigated the origins of Kerr phase and orientational phase in PDLC and their connection to two-step EO response. In our study, the Kerr phase is a result of LC orientation in the center of LC droplets. The orientational phase attribute to orientation of LC molecules near LC-polymer interfaces. The two phase in PDLC samples are adjustable depending on droplet size. We also found that two-steps EO response existing in small droplet (<333 nm) is related to Kerr phase and orientational phase. A modified PDLC model related to the Kerr phase and orientational phase is also proposed. Besides the conventional features of PDLC, such as polarization independent optical phase shift and response time independent of cell gap, we believe the Kerr phase and orientational phase with different response times (~ msec) in PDLC pave a way for designing versatile photonic devices with pure optical phase modulation.

**Keywords:** Liquid crystals, Kerr effect, Optoelectronics, Polymer dispersed liquid crystal, Optical phase modulation

## 1. INTRODUCTION

Polymer dispersed liquid crystal (PDLC) is an electro-optical material which modulates amplitude and phase of incident light. [1-8] Since the droplet size is close to wavelength of incident light, PDLC scatters the incident light by liquid crystal (LC) droplets that randomly dispersed in polymer matrix. [9-13] When a high electric field applies to PDLC, the scattering effect diminishes and optical phase modulation reveals because the incident light sees average refractive index in PDLC at high tilt angles of LC molecules with random orientations. [3, 14, 15] When the droplet size of PDLC is much smaller than wavelength of incident light, scattering effect vanishes and optical phase modulation with polarization independency remains. [15-17] In 1990, M. J. Sansone et. al. first discovered Kerr effect in PDLC, in which birefringence of PDLC is proportional to a square of electric field, by means of measurement of phase retardation in PDLC and proposed Kerr effect in PDLC originates from collective reorientation of the optically anisotropic liquid crystal micro-droplets, not electrically polarized LC molecules. [18] Thereafter, many researchers started to study Kerr effect of PDLC and attempted to enlarge Kerr constant in PDLC. [19-23] However, literatures reported that Kerr effect in PDLC might attribute to orientations of LC molecules, but no clear evidence could prove this up to now. [18] Instead of LC droplet in PDLC, structure of blue phase liquid crystals (BPLC) consisting of double twisted cylinders also exhibits Kerr effect. [24-27] In 2012, we first experimentally demonstrated the orientation of LC molecules giving rise to Kerr effect of BPLC by analyzing optical phase of BPLC and transmittance of dye-doped BPLCs. [27]

\* yilin@mail.nctu.edu.tw; phone +886-3-5712121-56376; fax +886-3-5716631; <http://web.it.nctu.edu.tw/~yilin/en/index.html#>

Moreover, two-steps electro-optical (EO) response in PDLC is still controversial. [28] Doane et al. firstly delineated experimental results of two-steps of the electro-optical (EO) response (i.e. two slopes in response time) of PDLC based on a measurement of amplitude modulation.[1] Later on, Drzaic [28] and Jain et al. [29] reported similar phenomena. Later on, Drzaic proposed a possible explanation of two-steps EO response: When small electric field applies to PDLC, LC molecules located in the middle of a droplet start to re-orientate because the anchoring energy near the boundary is rather high. When high electric fields apply to PDLC, LC molecules near boundary (i.e. interface between polymer and LC) of a droplet are also re-oriented by electric fields due to the electric force overcomes the anchoring force. The anchoring energy or so-called “elastic deformation free energy” is provided by LC-polymer elliptical interface. [9-11, 16, 28, 30] However, the explanation does not apply to PDLCs without the two-step EO response. How Kerr effect plays the role in two-steps EO response still needs to be investigated. Instead of amplitude modulation of PDLC, L. Vicari presented a mathematical model for optical phase of PDLC based on order parameters of LC molecules and the model predicted optical phase in nano-PDLC which agreed well with experiments. [31] However, L. Vicari did not discuss two-steps EO response as well as Kerr effect in PDLC. Recently, we demonstrated electrically tunable focusing microlens arrays of nano-PDLC with polarization independency. [32] We ascribe the polarization-independent phase to the orientational phase as well as Kerr phase induced by Kerr effect. Meanwhile, the phase shift of Kerr phase was small compared to the orientational phase shift. From above, it all motivates us to investigate that the origins of Kerr phase and orientational phase in PDLC, and study how those two phases involve in two-steps EO responses.

In this paper, we investigated the origins of Kerr phase and orientational phase of PDLC as well as the connection between two optical phases and two-steps EO response. We prepared PDLC samples with different droplet sizes and we analyzed data obtained from measurement of transmittance, optical phase shifts and EO response. From the analysis of experimental results, the Kerr phase is a result of LC orientations in the middle of a droplet, which leads to a linear optical phase shift proportional to a square of electric field. The orientational phase is a major contribution of the orientation of LC molecules near LC-polymer interfaces. The amount of Kerr phase and orientational phase in PDLC samples are depending on droplet size. We also found that two steps EO response only exists in small droplet (<333 nm). The two-steps EO response indeed related to Kerr phase and orientational phase. The Kerr phase and orientational phase in PDLC lead us to propose a modified PDLC model. Two kinds of optical phase shifts with different response times in PDLC would help researchers to design photonic devices with pure optical phase modulation, such as LC lenses and laser beam steering.

## 2. EXPERIMENTS

### 2.1 Sample preparation

The PDLC mixtures were made of nematic liquid crystals (Merck, MLC-2053,  $n_e=1.7472$ ,  $n_o=1.5122$ ,  $\Delta n=0.235$ ,  $\Delta\epsilon=42.6$ ,  $T_{NI}=86^\circ\text{C}$ ), NOA65 (a UV curable prepolymer, Norland) and photo-initiator (Irgacure 907). The weight percentage of the mixtures were 35 wt% (LC) : 64 wt% (NOA65) : 1 wt% (Irgacure 907) for sample A, 40 wt% (LC) : 59 wt% (NOA65) : 1 wt% (Irgacure 907) for sample B, 50 wt% (LC) : 49 wt% (NOA65) : 1 wt% (Irgacure 907) for sample C, and 55 wt% (LC) : 44 wt% (NOA65) : 1 wt% (Irgacure 907) for sample D. The mixtures were heated to  $88^\circ\text{C}$  and stirred for 1 hour. The empty cells were made of two indium-tin-oxide (ITO) coated glass substrates separated with dispersed ball spacers (diameter of  $20\ \mu\text{m}$ ). After filled with the mixtures, the cells were cooled down to  $26^\circ\text{C}$  and then exposed to UV light ( $\lambda=365\text{nm}$ ,  $I=200\ \text{mW}/\text{cm}^2$ ) for 1 minutes for polymerization. The thermal fluctuation were well prevented during the polymerization process by covering the stage with a cardboard box.

### 2.2 Morphology

A scanning electron microscopy (SEM) was applied to observe the morphologies of the samples. After soaked in hexane for 48 hours to remove the liquid crystals, the samples were coated with platinum by sputtering (10 mA, 90 sec) in order to enhance the conductivity. Electron beams with an energy of 5 kV were injected into the samples to obtain SEM images. The SEM images showed that the samples consist of droplets dispersed in the polymer matrix with LCs filling the voids. The SEM images were analyzed by Image J, a Java-based image-processing program developed at the National Institutes of Health. The average droplet sizes  $d_{\text{drop}}$  of samples A, B, C, and D are 176, 220, 333, and 483 nm, respectively. We defined the filling factors as the ratios between the area occupied by droplets and the entire area in SEM area. The values of the four samples were 5.6%, 8.6%, 17.3%, and 20.4% for samples A, B, C, and D, respectively. The volume fraction  $\eta_v$  was calculated by the formula:

$$\eta_V = \frac{4\pi}{3}(F/\pi)^{3/2} \quad (1)$$

F is the filling factor. The volume fractions of samples A, B, C, and D were 1%, 1.9%, 5.4%, and 6.9%, respectively. As shown in Fig. 1., both the droplet size and the volume fraction increase linearly with the liquid crystal concentration in four PDLC samples. However, these values are approximately one-tenth of those calculated from the weight percentage, which are 43%, 49%, 62%, and 68%, respectively. This is probably because some of the LCs are dissolved in the polymer matrix.

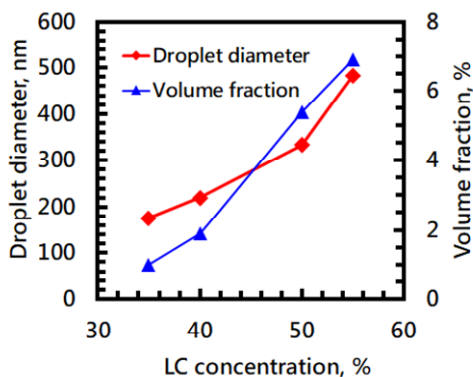


Fig. 1. Average droplet diameter and volume fraction as functions of LC concentration.

### 2.3 Transmittance

In order to verify the scattering effects in PDLC samples, we measured the transmittance of the samples. The samples were irradiated by an unpolarized He-Ne laser (JDSU, Model 1122,  $\lambda = 633$  nm) at normal incidence, and a photodetector (New Focus, Model 2031) was placed 25 cm from the samples to measure the transmitted light while a voltage  $V$  was applied to the samples. Fig. 2 shows the transmittance of the samples as a function of applied voltage. The transmittances at  $V = 0$  are 87%, 82%, 63%, and 50% for samples A, B, C, and D, respectively. The transmittance increased with increasing applied voltage when the voltage exceeded the threshold voltages ( $V_{th}$ ), which were  $\sim 15 V_{rms}$  (sample A),  $\sim 16 V_{rms}$  (sample B),  $\sim 10 V_{rms}$  (sample C), and  $\sim 8 V_{rms}$  (sample D). The threshold voltage is reportedly proportional to  $1/\sqrt{D}$ , where  $D$  is the diameter of the LC droplets [33]. The data for our samples fit this relationship with a correlation coefficient of 0.82. Above certain voltages, the transmittance of all the samples saturates at a value exceeding 90%.

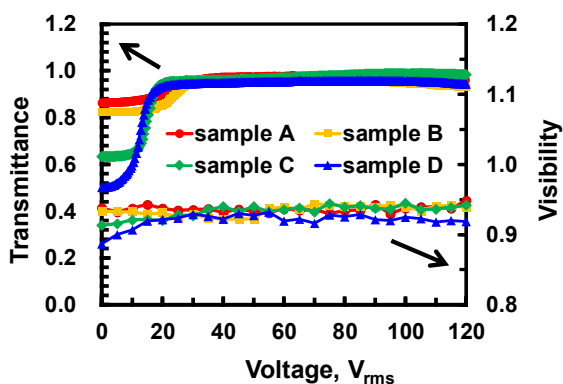


Fig. 2. Transmittance and visibility as functions of an applied voltage.

### 2.4 Optical phase shift

The optical phase shift and interference fringes were measured and recorded by a Mach-Zehnder interferometer with a two-arm configuration [34]. The samples were placed in one of the arms of the interferometer, and the interference

fringes were recorded by a digital camera (Sony, RX100 M3) while different voltage is applied to the samples. The interference fringes were then analyzed by Matlab.

To identify the whether the scattering affected the optical phase modulation, we analyzed the visibility of the interference fringes. The visibility of the fringes is defined as the ratio of  $(I_{\max} - I_{\min})$  to  $(I_{\max} + I_{\min})$ , where  $I_{\max}$  and  $I_{\min}$  are the maximum and minimum irradiance of the fringes, respectively. Since the fringes are recorded by digital camera, which the relation between tristimulus values and the intensity is nonlinear, the intensity of each pixel should be applied to Gamma correction. With a typical gamma value 2.2, the correction formula was

$$I = (T / 255)^{2.2} \quad (2)$$

T was the tristimulus value recorded by camera. Fig. 2 shows the visibility of the four samples as a function of applied voltage. The visibilities of samples A and B (~0.93) are similar to the visibility of fringes without a sample (~0.92). The visibility of sample C is approximately 0.91 at  $V = 0$ , and that of sample D is slightly lower, ~0.88. Compared to the fringe visibility of ~0.92 with no sample, the scattering in samples A, B, and C did not affects the fringe visibility. This indicated nearly pure optical phase modulation occurs under the applied voltage. Fig. 1 also provides supporting evidence in terms of the droplet sizes of samples A, B, and C, which are smaller than the laser wavelength. The visibility is less than 1 because of the coherent properties of the laser. For sample D, the size of the droplets were close to the laser wavelength. Despite the strong scattering effect, the visibility of the fringe is still high enough to obtain optical phase modulation. The low transmittance of the samples at  $V = 0$  in Fig. 2 can also be partially attributed to multiple Fresnel reflections and refractions at the interfaces resulting from the refractive index difference between the LC and the polymer.

The optical phase shift of the PDLC samples was converted from the fringe shift when a voltage V is applied to the samples. Fig. 3 shows the optical phase shift as a function of applied voltage on the samples. The total optical phase shifts were  $0.277\pi$  radians (sample A),  $0.455\pi$  radians (sample B),  $0.865\pi$  radians (sample C), and  $1.157\pi$  radians (sample D). Different from the transmittance response in fig. 2, the optical phase shift response showed no threshold features. In addition, We discovered that the optical phase shift response while the applied voltage is below transmittance threshold voltage ( $V < V_{th}$ ) is proportional to the square of applied voltage. The behavior of such phase modulation is similar to Kerr effect. Thus, we defined this portion of the optical phase shift as Kerr phase. The maximum Kerr phase of the samples at  $V = V_{th}$  are  $0.08\pi$  radians (sample A),  $0.092\pi$  radians (sample B),  $0.271\pi$  radians (sample C), and  $0.53\pi$  radians (sample D). On the other hand, the optical phase shift when the voltage is higher threshold voltage ( $V > V_{th}$ ) deviated from the linearity to the square of applied voltage. We defined the phase as orientational phase.

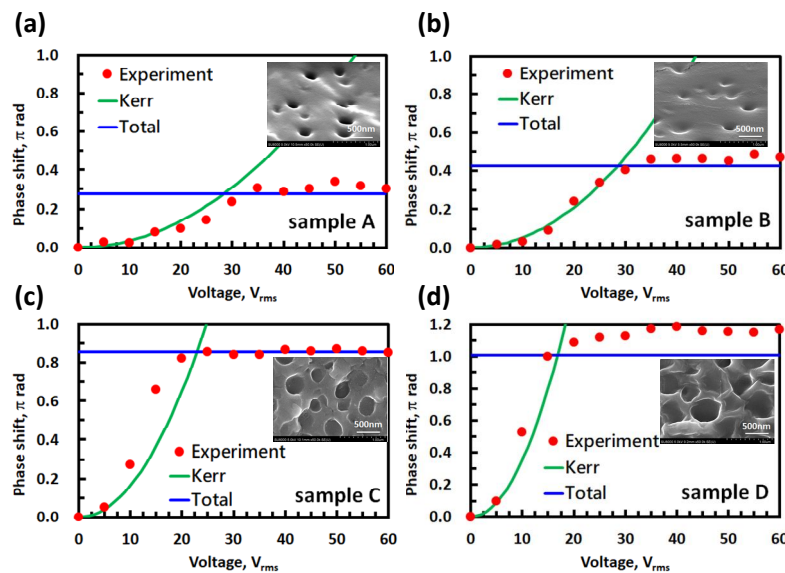


Fig. 3. Phase shift as a function of applied voltage ( $\lambda = 633$  nm). Red dots are experimental results; red lines are the Kerr phase base on theoretical calculation; blue lines are theoretical total phase shift.

## 2.5 Phase shift response

To examine the phase shift response time of the PDLC samples, we measured the fringe shift as a function of time using a Mach-Zehnder interferometer. A saturate voltage of  $40 V_{rms}$  (1 kHz) was applied to the samples and then turned off. A

photodetector (New Focus, Model 2031) replaced the digital camera in the setup of optical phase shift measurement and the signal was sent to an oscilloscope to record the rising and relaxing optical response. The recorded optical responses were then converted to normalized optical phase shifts. Fig. 4 (a) illustrates the rising phase shift as a function of time, where we turned the voltage on at  $t = 1$ . The rise times, which is defined as the time duration between start time and saturation time, were 5.15 ms (sample A), 1.74 ms (sample B), 1.52 ms (sample C), and 1.45 ms (sample D). Typically, rise time of PDLC depends on applied voltage and threshold voltage. Thus, sample A with the highest threshold voltage ( $V_{th} = 15 \text{ V}_{rms}$ ) has the longest rise time. Fig. 4 (b) shows the relaxation phase shift as a function of time, where we turned the voltage off at  $t = 1$ . Interestingly, we found significant two steps in the response of all samples. The response times of the first step were 3.68 ms, 2.89 ms, 4.82, and 8.66 ms for sample A, B, C, and D respectively. As for the second step, they were 4.42 ms, 4.5 ms, 8.53ms, and 8.51 ms for sample A, B, C, and D respectively.

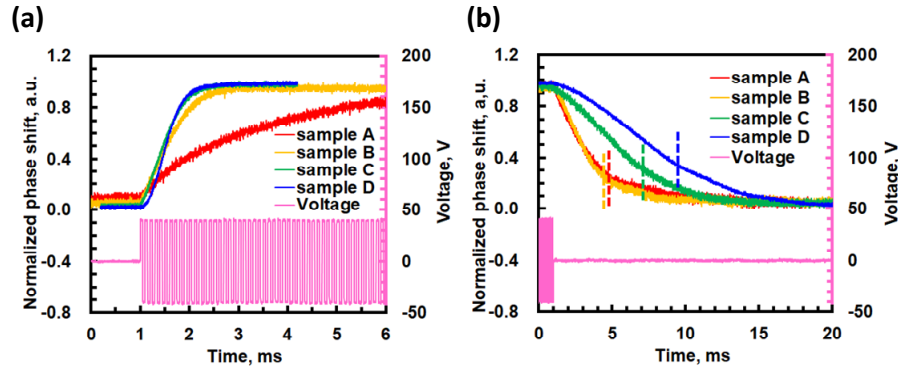


Fig. 4. Optical phase shift of the samples as a function of time, where the voltage ( $40 \text{ V}_{rms}$ ) was turned on and off at  $t = 1$ . Pink lines are the applied voltage signals. Dotted lines are the divides of two steps of response.

### 3. DISCUSSION

To figure out the mechanism of the Kerr phase and orientation phase, we assumed that all the phase shift is due to the liquid crystal reorientation induced by electric force. From the average droplet diameters and filling factors of the samples that we obtained from SEM pictures, we calculated the total optical phase shift ( $\Delta\phi_{theory}$ ) of the samples at  $V \gg V_{th}$  according to

$$\Delta\phi_{theory}(V) = \Delta n'(V) \times \frac{2\pi}{\lambda} \times d \times F \quad (3)$$

Where  $F$  is the filling factor,  $d$  is the sample thickness ( $20 \mu\text{m}$ ), and  $\Delta n'$  is the difference between average refractive index [ $n_{avg}(V)$ ] at a particular voltage and the refractive index at  $V = 0$ , which can be written as  $\Delta n'(V) \sim \frac{n_e - n_o}{3}$ . The

calculated results were plotted as the blue lines in Fig. 3. The line matched the maximum phase shift in all the samples, which indicated that both Kerr phase and orientation phase are both ascribed to LC molecule reorientation.

The difference between Kerr phase and orientation phase is the linearity to the square of electric field. To evaluate the linearity of the Kerr phase, we wrote the Kerr phase as a function of refractive index difference

$$\Delta\phi_{Kerr}(V) = \frac{2\pi \times d \times F}{\lambda} \times \Delta n_{Kerr}(V). \quad (4)$$

Where  $F$  is the filling factor,  $d$  is the sample thickness ( $20 \mu\text{m}$ ), and  $\Delta n_{Kerr}(V)$  is the birefringence induced by Kerr effect, which can be written as  $\Delta n_{Kerr}(V) = \lambda \times K \times E(V)^2$ .  $K$  is defined as Kerr constant. From Eq. (4) and the Kerr phases at  $V = V_{th}$ , we can calculate the Kerr constant:  $6.15 \times 10^{-8} \text{ m/V}^2$  (sample A),  $6.13 \times 10^{-8} \text{ m/V}^2$  (sample B),  $9.44 \times 10^{-8} \text{ m/V}^2$  (sample C), and  $1.74 \times 10^{-7} \text{ m/V}^2$  (sample D). From the calculated Kerr constant, we plotted the theoretical Kerr phase  $\Delta\phi_{Kerr}$  (green line) with the measured phase shift (red dots) in Fig. 4. The measured phase shift matches the theoretical Kerr phase when applied voltage is lower than threshold voltage  $V < V_{th}$ . The Kerr constants of our samples are on the order of  $\sim 10^{-7} - 10^{-8} \text{ m/V}^2$ . The electric-field-induced birefringence of the samples ranges from 0.015 to 0.25, which is similar in order of magnitude to results reported in the literature ( $\sim 0.025$ ) [18]. We further calculated the

average refractive index [ $n_{\text{ave}}(V_{\text{th}})$ ] of the samples at  $V = V_{\text{th}}$ . Here  $n_{\text{ave}}(V_{\text{th}})$  is equal to  $\Delta n_{\text{ker}} r(V_{\text{th}}) + n_i$ , where  $n_i$  is the average refractive index at  $V = 0$ ;  $n_i = (n_e + 2n_o) / 3 \sim 1.59$ , assuming the LC droplets are randomly dispersed in the polymer matrix. As a result,  $n_{\text{ave}}(V_{\text{th}})$  is 1.612, 1.615, 1.605, and 1.608 for samples A, B, C, and D. The results show that the LC molecules in sample D are more highly oriented than those in sample A. This is reasonable because LC molecules are more difficult to reorient in a small droplet.

To investigate the EO response of the samples, we fitted Fig. 4 (b) using Origin software (OriginLab Corp.). Assuming conventional Debye relaxation [35–37], we fitted the EO response using a combination of two exponential functions:  $P(t) = a \cdot \exp^{-(t-\tau_1)/\tau_1} + b \cdot \exp^{-(t-\tau_2)/\tau_2}$ .  $P(t)$  represents the two-step EO response and normalized optical phase shift at a certain time ( $t$ );  $a$  and  $b$  are normalized Kerr and orientational phase obtained from the phase shift measurement; and  $\tau_1$  and  $\tau_2$  are the time delays of the two relaxation responses.  $\tau_1$  and  $\tau_2$  represent the time constants of the two relaxation responses which are fitting parameters. The relation between time constant ( $\tau_1$  and  $\tau_2$ ) and LC droplet diameter is further analyzed. Fig. 5 shows the time constant and the analysis results as function of droplet size. The black dots are the ratio between two time constants, which shows that there is no difference between them in samples C and D. This means there is only one Debye relaxation in sample C and D. The red triangles and blue squares are time constants of first and second step respectively. We found that  $\tau_1 \sim d_{\text{drop}}^{2.2}$  and  $\tau_2 \sim d_{\text{drop}}^{1.46}$  ( $\tau_2$  was fitted only for  $d_{\text{drop}} > 333$  nm). As a result, we can say that the first step of the EO response is similar to the nematic relaxation in Eq. (3) (i.e.,  $\tau_{\text{off}} \sim a^2$ ). We conclude that the first step of the EO response is related to the orientational phase, and the second step is related to the Kerr phase.

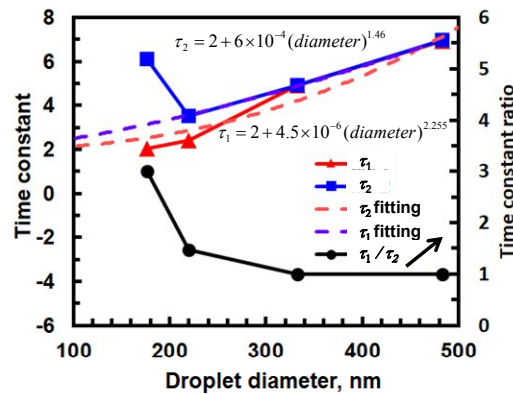


Fig. 5. Time constants as a function of droplet size. Red triangles are the first response step. Blue squares are the second response step. Dotted line are the fitting curve of the two time constants. Black dots are the ratio between the two time constants.

Moreover, the orientational phase responds more quickly than the Kerr phase ( $\tau_1 < \tau_2$ ) for  $d_{\text{drop}} < 333$  nm due to strong anchoring force from the LC-polymer boundary. For photonic devices with purely optical phase operation, PDLCs that provide two types of optical phase shifts with different response times can be obtained by adjusting the droplet size.

From the experimental results and analysis above, we schematically illustrate the Kerr phase and orientational phase of the PDLCs in Figs. 6. For PDLCs with small LC droplets (<333 nm), the symmetric axes of LC droplets with bipolar configurations are randomly distributed in the polymer matrix [Fig. 6 (a)]. When  $V < V_{\text{th}}$ , the LC molecules at the centers of the LC droplets are reoriented by the electric field, while the LC molecules at the edge is anchored due to the non-spherical LC-polymer interface. As a result, we obtain an optical phase shift that is linearly proportional to the square of the electric field, called the Kerr phase [Fig. 6 (b)]. When  $V > V_{\text{th}}$ , the linearity of this optical phase shift is destroyed because more LC molecules in the droplet are aligned parallel to the electric field. The nonlinear optical phase shift at  $V > V_{\text{th}}$  is the orientational phase [Fig. 6 (c)]. According to the PDLC model of Drzaic [9, 28], the bipolar defects of the droplets are stable when  $V < V_{\text{th}}$  but rotate when  $V > V_{\text{th}}$  to minimize the elastic energy. For PDLCs with large LC droplets (>333 nm), there is a similar random distribution of LC droplets. Because the LC droplets are large, it is relatively easy for LC molecules, including their bipolar point defects, to be reoriented by an applied electric field. Thus, we obtained only one step EO response, which is the result of point defect rotation as the voltage turns on. For small LC droplets, the orientational phase relaxes more rapidly than the Kerr phase. This indicates that relaxation of bipolar point defects occurs more quickly. Instead of explaining the Kerr effect in PDLCs as originating from collective reorientation of the optically anisotropic LC microdroplets, as proposed by Sansone et al. [18], we provide a more insightful and elaborate model related to the Kerr phase. Compared to conventional light intensity measurement, optical phase measurement using a sensitive interferometer provides more information related to the LC orientation.

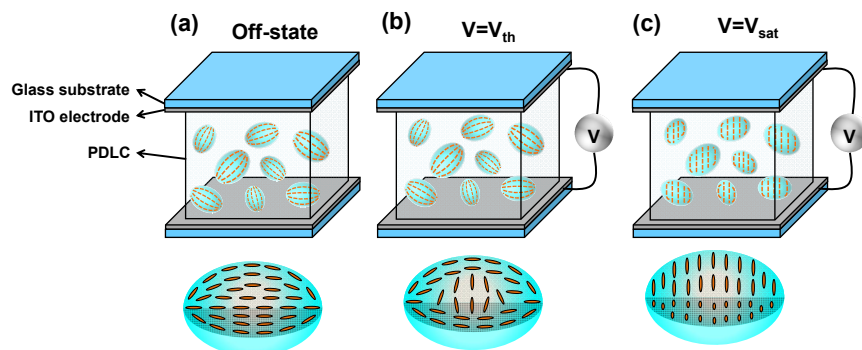


Fig. 6 Kerr and orientational phases in PDLC with small LC droplets.

#### 4. CONCLUSION

Based on experiments, we investigated the origins of Kerr phase and orientational phase in PDLC as well as the correlation between two optical phases and two-steps EO response. The Kerr phase, linearly proportional to a square of electric field, is a result of LC orientations in the middle of a droplet. The orientational phase is a contribution of the orientation of LC molecules near LC-polymer interfaces. The Kerr phase and orientational phase in PDLC samples are adjustable depending on droplet size. We also found that two-steps EO response existing in small droplet (<333 nm) indeed related to Kerr phase and orientational phase. Rotations of point defects play a role in EO responses. A modified PDLC model related to the Kerr phase and orientational phase is proposed as well. The proposed theoretical model being phenomenological captures the main features of the Kerr phase and may be used to optimize the PDLC film properties. Besides the conventional features of PDLC, such as polarization independent optical phase shift and response time independent of cell gap, we believe the Kerr phase and orientational phase with different response times ( $\sim$  msec) in PDLC pave a way for designing versatile photonic devices with pure optical phase modulation.

#### REFERENCES

- [1] J. W. Doane, N. A. Vaz, B. G. Wu, and S. Zumer, "Field controlled light scattering from nematic microdroplets," *Appl. Phys. Lett.* **48**(4), 269-271 (1986).
- [2] J. Ferguson, "Polymer encapsulated nematic liquid crystals for display and light control applications," *Soc. Inf. Disp. Int. Symp. Dig. Tech. Pap.* **16**, 68 (1985).
- [3] P. Chanclou, B. Vinouze, M. Roy, and C. Cornu, "Optical fibered variable attenuator using phase shifting polymer dispersed liquid crystal," *Opt. Commun.* **248**(1-3), 167-172 (2005).
- [4] C. Levallois, B. Caillaud, J. de Bougrenet de la Tocnaye, L. Dupont, A. Lecorre, H. Folliot, O. Dehaese, and S. Loualiche, "Nano-polymer-dispersed liquid crystal as phase modulator for a tunable vertical-cavity surface-emitting laser at 1.55  $\mu\text{m}$ ," *Appl. Opt.* **45**, 8484-8490 (2006).
- [5] H. W. Ren, Y. H. Fan, Y. H. Lin, and S. T. Wu, "Tunable-focus microlens arrays using nanosized polymer-dispersed liquid crystal droplets," *Opt. Commun.* **247**, 101-106 (2005).
- [6] S. Massenot, R. Chevallier, J.-L. de Bougrenet de la Tocnaye, and O. Parriaux, "Tunable grating-assisted surface plasmon resonance by use of nano-polymer dispersed liquid crystal electro-optical material," *Opt. Commun.* **275**, 318-323 (2007).
- [7] S. G. Kang and J. H. Kim, "Optically-isotropic nanoencapsulated liquid crystal displays based on Kerr effect," *Opt. Express* **21**, 15719-15727 (2013)
- [8] S. S. Gandhi and L. C. Chien, "High transmittance optical films based on quantum dot doped nanoscale polymer dispersed liquid crystals," *Opt. Mater.* **54**, 300-305 (2016).
- [9] P. S. Drzaic, [Liquid Crystal Dispersions], World Scientific, Singapore, 183-338 (1995).
- [10] F. Simoni, [Nonlinear Optical Properties of Liquid Crystals and Polymer Dispersed Liquid Crystals], World Scientific, Singapore, 176-250 (1997)
- [11] D. K. Yang and S. T. Wu, [Fundamentals of Liquid Crystal Devices], John Wiley & Sons, 363-409 (2006).
- [12] S. Zumer and J. W. Doane, "Light scattering from a small nematic droplet," *Phys. Rev. A* **34**(4), 3373 (1986).



- [13] S. Zumer. "Light scattering from nematic droplets: Anomalous-diffraction approach," *Phys. Rev. A* **37**(10), 4006 (1988).
- [14] H. Ren, Y. H. Lin, Y. H. Fan, and S. T. Wu, "Polarization-independent phase modulation using a polymer-dispersed liquid crystal," *Appl. Phys. Lett.* **86**, 141110 (2005).
- [15] G. B. Hadjichristov, Y. G. Marinov, and A. G. Petrov, "Gradient polymer-disposed liquid crystal single layer of large nematic droplets for modulation of laser light," *Appl. Opt.* **50**, 2326-2333 (2011).
- [16] D. E. Lucchetta, R. Karapinar, A. Manni, and F. Simoni, "Phase-only modulation by nanosized polymer-dispersed liquid crystals," *J. Appl. Phys.* **91**(9), 6060-6065 (2002).
- [17] F. Basile, F. Bloisi, L. Vicari, and F. Simoni, "Optical phase shift of polymer-dispersed liquid crystals," *Phys. Rev. E* **48**(1), 432 (1993).
- [18] M. J. Sansone, G. Khanarian, T. M. Leslie, M. Stiller, J. Altman, and P. Elizondo, "Large Kerr effects in transparent encapsulated liquid crystals," *J. Appl. Phys.* **67**, 4253-4259 (1990).
- [19] S. W. Choi, S. I. Yamamoto, Y. Haseba, H. Higuchi, and H. Kikuchi, "Optically isotropic-nanostructured liquid crystal composite with high Kerr constant," *Appl. Phys. Lett.* **92**, 043119 (2008).
- [20] S. Aya, K. V. Le, F. Araoka, K. Ishikawa, and H. Takezoe, "Nanosize-induced optically isotropic nematic phase," *Jpn. J. Appl. Phys.* **50**, 051703 (2011).
- [21] J. Niziol, R. Weglowski, S. J. Klosowicz, A. Majchrowski, P. Rakus, A. Wojciechowski, I. V. Kityk, S. Tkaczyk, and E. Gondek, "Kerr modulators based on polymer-dispersed liquid crystal complexes," *J. Mater. Sci. Mater. Electron.* **21**(10), 1020-1023 (2010).
- [22] R. Weglowski, S. J. Klosowicz, A. Majchrowski, S. Tkaczyk, A. H. Rechak, J. Pisarek, and I. V. Kityk, "Enhancement of the Kerr response in polymer-dispersed liquid crystal complexes due to incorporation of  $\text{BiB}_3\text{O}_6$  nanocrystallites," *Mater. Lett.* **64**, 1176-1178 (2010).
- [23] M. Jiao, J. Yan, and S. T. Wu, "Dispersion relation on the Kerr constant of a polymer-stabilized optically isotropic liquid crystal," *Phys. Rev. E* **83**, 041706 (2011).
- [24] H. Kikuchi, M. Yokota, Y. Hisakado, H. Yang, and T. Kajiyama, "Polymer-stabilized liquid crystal blue phases," *Nat. Mater.* **1**, 64-68 (2002).
- [25] J. Yan, H. C. Cheng, S. Gauza, Y. Li, M. Jiao, L. Rao, and S. T. Wu, "Extended Kerr effect of polymer-stabilized blue-phase liquid crystals," *Appl. Phys. Lett.* **96**, 071105 (2010).
- [26] K. M. Chen, S. Gauza, H. Xianyu, and S. T. Wu, "Hysteresis effects in blue-phase liquid crystals," *J. Disp. Technol.* **6**, 318-322 (2010).
- [27] H. S. Chen, S. Y. Ni, and Y. H. Lin, "An experimental investigation of electrically induced-birefringence of Kerr effect in polymer-stabilized blue phase liquid crystals resulting from orientations of liquid crystals," *Appl. Phys. Lett.* **101**, 093501 (2012).
- [28] P. S. Drzaic, "Reorientation dynamics of polymer dispersed nematic liquid crystal films," *Liq. Cryst.* **3**(11), 1543-1559 (1988).
- [29] S. C. Jain and D. K. Rout, "Electro-optic response of polymer dispersed liquid-crystal films," *J. Appl. Phys.* **70**(11), 6988-6992 (1991).
- [30] B. G. Wu, J. H. Erdmann, and J. W. Doane, "Response times and voltages for PDLC light shutters," *Liq. Cryst.* **5**(5), 1453-1465 (1989).
- [31] L. Vicari, "Electro-optic phase modulation by polymer dispersed liquid crystals," *J. Appl. Phys.* **81**(10), 6612-6615 (1997).
- [32] J. H. Yu, H. S. Chen, P. J. Chen, K. H. Song, S. C. Noh, J. M. Lee, H. Ren, Y. H. Lin, and S. H. Lee, "Electrically tunable microlens arrays based on polarization-independent optical phase of nano liquid crystal droplets dispersed in polymer matrix," *Opt. Express* **23**, 17337-17344 (2015).
- [33] V. Y. Reshetnyak, T. J. Sluckin, and S. J. Cox, "Effective medium theory of polymer dispersed liquid crystal droplet systems: II. Partially oriented bipolar droplets," *J. Phys. D: Appl. Phys.* **30**, 3253-3266 (1997).
- [34] J. Yan, M. Jiao, L. Rao, and S. T. Wu, "Direct measurement of electric-field-induced birefringence in a polymer-stabilized blue-phase liquid crystal composite," *Opt. Express* **18**(11), 11450-11455 (2010).
- [35] R. G. Palmer, D. L. Stein, E. Abrahams, and P. W. Anderson, "Models of hierarchically constrained dynamics for glassy relaxation," *Phys. Rev. Lett.* **53**(10), 958-961 (1984).
- [36] J. C. Philips, "Stretched exponential relaxation in molecular and electronic glasses," *Rep. Prog. Phys.* **59**, 1133-1207 (1996).
- [37] I. C. Khoo and S. T. Wu, [Optics and Nonlinear Optics of Liquid Crystals], World Scientific, Singapore, 1010-258 (1993).